Supplementary Material

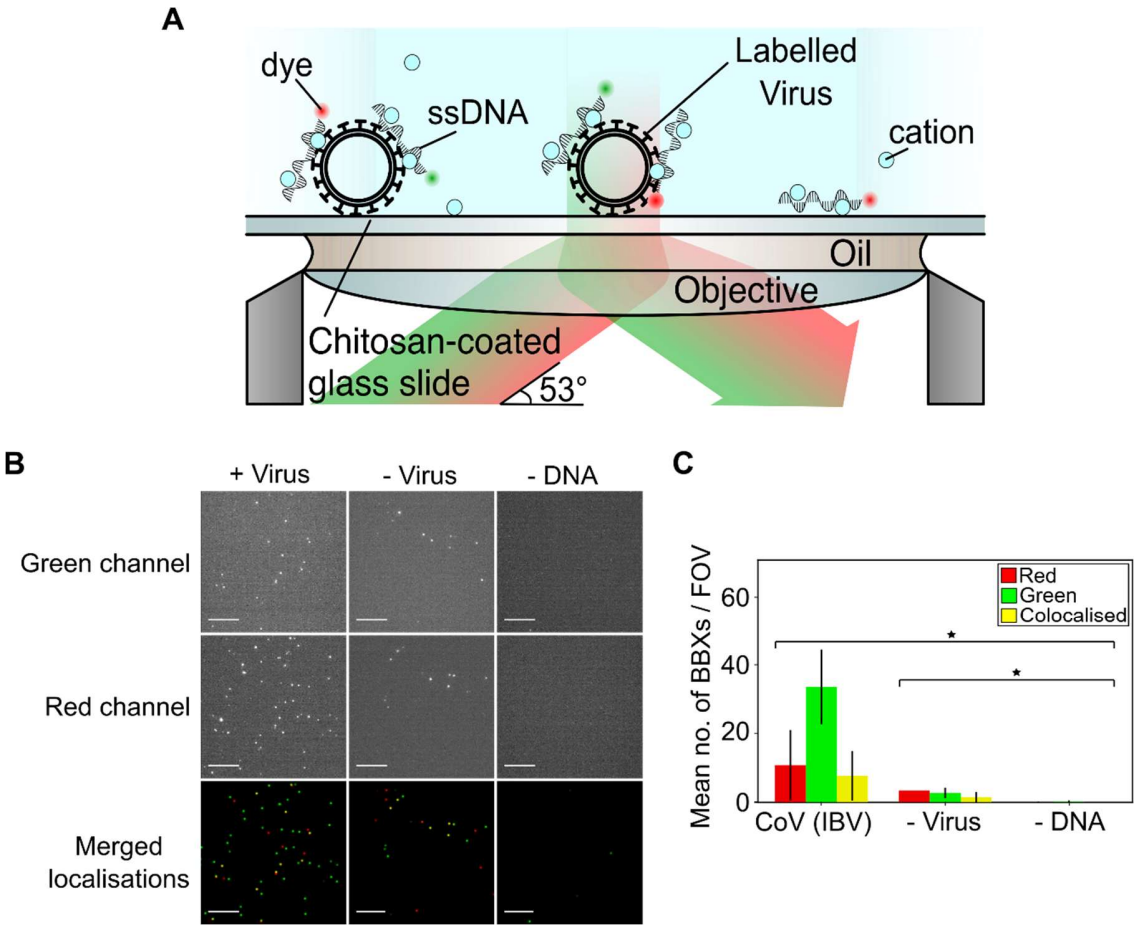

Sup. Fig. 1. Schematic of virus labelling and immobilisation strategy. Positively charged cations (e.g. calcium, strontium) bridge the lipid membrane of the virus and the negatively charged phosphate groups on the ssDNA, binding fluorescently labelled ssDNA to the surface of the virus. Labelled viruses were immobilised on a chitosan-coated glass slide and illuminated with red and green laser light on a widefield Total Internal Reflection Fluorescence (TIRF) microscope. B) Representative fields of view (FOVs) of fluorescently labelled infectious bronchitis virus (CoV (IBV)). The virus sample, at a final concentration of $1x10^4$ PFU/mL, was immobilized and labelled with 0.23 M $CaCl_2$, 1 nM Cy3 (green) DNA and 1 nM Atto647N (red) DNA before being imaged. Green DNA was observed in the green channel (top panels) and red DNA in the red channel (middle panels); merged red and green localisations are shown in the lower panels. Scale bar 10 µm. A negative control where DNA was replaced with water is included. C) Plot showing the mean number of BBXs per FOV for labelled CoV (IBV) and the negative controls. Error bars represent the standard deviation of 81 FOVs from one slide. Statistical significance was determined by one-way ANOVA, *P<0.0001.

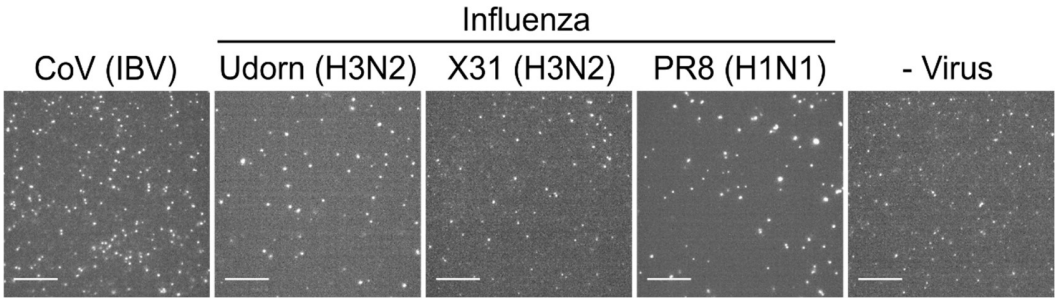

Sup. Fig. 2. TIRF images of four different viruses. Representative fields of view (FOVs) of fluorescently labelled CoV (IBV), influenza A (Udorn, X31 and PR8) and a virus-negative control (- Virus). The samples were immobilized and labelled with 0.23 M $SrCl_2$, 1 nM Cy3 (green) DNA and 1 nM Atto647N (red) DNA before being imaged. FOVs from the red channel are shown. Scale bar 10 µm.

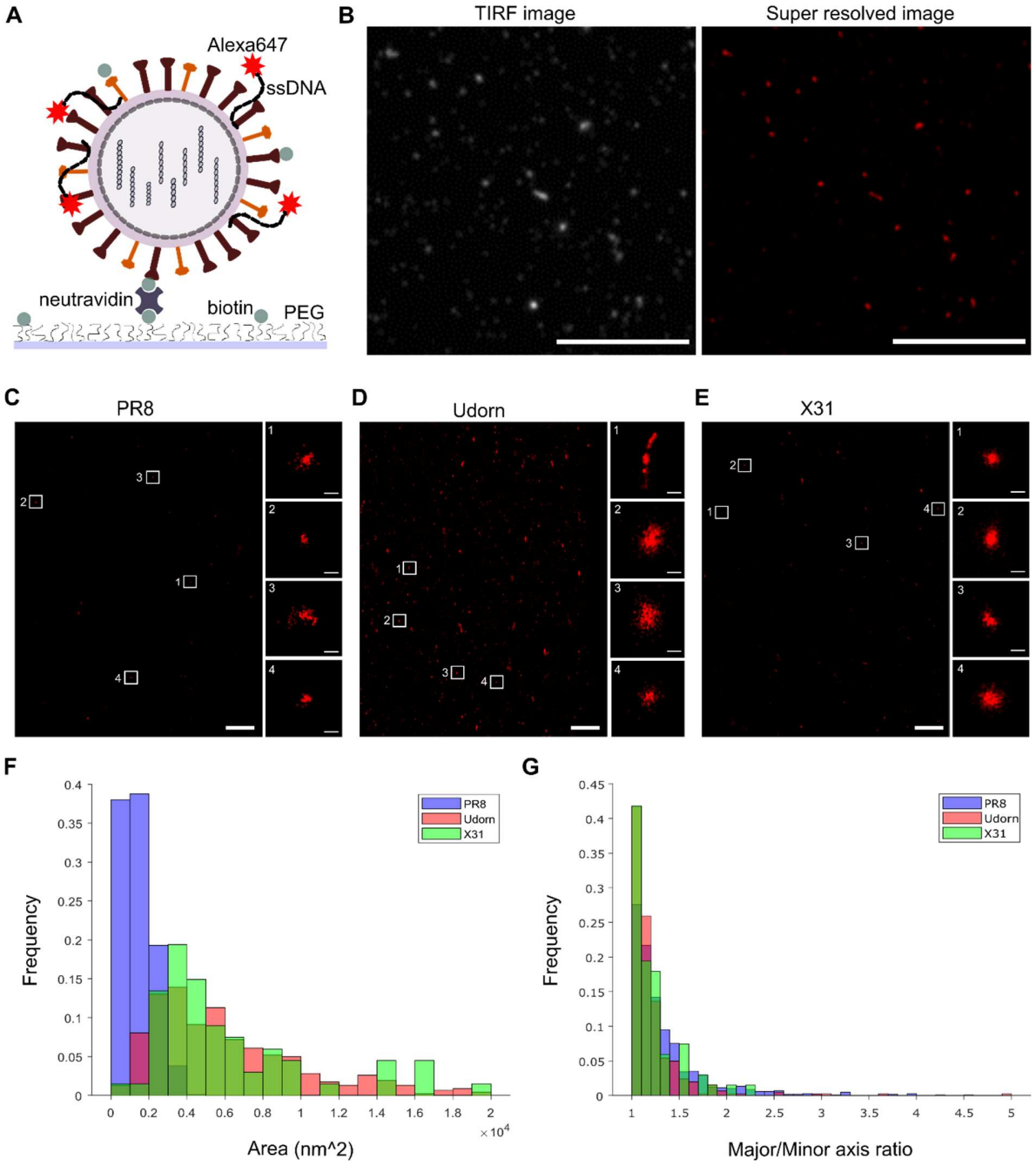

Sup. Fig. 3 Super resolution images of cation-labelled virus particles. A) Schematic of immobilisation scheme. Virus particles were biotinylated and subsequently labelled with 0.23 M $CaCl_2$ and 1 nM DNA with a photoswitchable Alexa647 dye. The labelled, biotinylated virus was incubated on a biotin-PEG slide that had been treated with neutravidin, imaging buffer was added and the slide was imaged. B) Representative diffraction-limited TIRF FOV and the corresponding super-resolved image. C) Representative super-resolved image of immobilised PR8 virus. Scale bar 10 µm. White squares highlight zoomed in particles shown to the right, scale bar 100 nm. D) As in C) but for Udorn virus. E) As in C) but for X31 virus. F) Histogram of the areas of PR8, Udorn and X31 (extracted from 4 FOVs of PR8, 2 FOVs of Udorn and 1 FOV of X31). G) Histogram of the major/minor axis ratio of PR8, Udorn and X31.

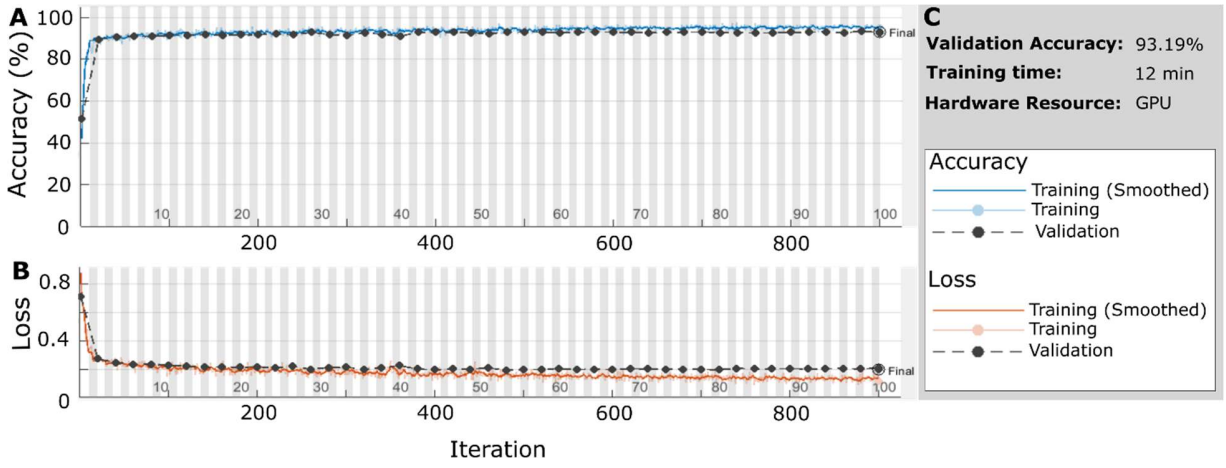

Sup. Fig. 4 Training Progress for CoV (IBV) and the virus-negative control (- Virus). A) Graph describing the validation accuracy of the network per iteration. B) Graph showing the loss function value for each iteration. C) Overall validation accuracy and training time.

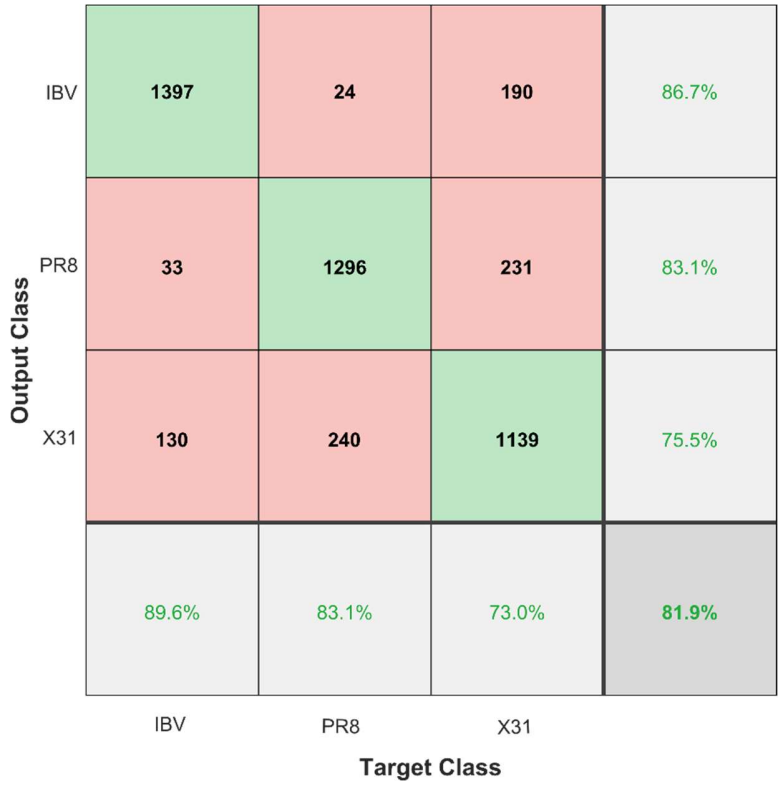

Sup. Fig. 5. Multi-classifier network validation results for laboratory-grown virus strains. Confusion matrix showing that a trained network could differentiate between three virus strains (the coronavirus IBV and two influenza strains, PR8 and WSN). 5200 BBXs were obtained for each strain and were then randomly divided into a training dataset (70%) and a validation dataset (30%). The training dataset was used to train the multi-classifier CNN to differentiate IBV from PR8 from WSN. The trained network was validated using the remaining 30% of the data and the results depicted in the confusion matrix. IBV is easily distinguishable from the two influenza strains, which can also be distinguished from each other with high accuracy.

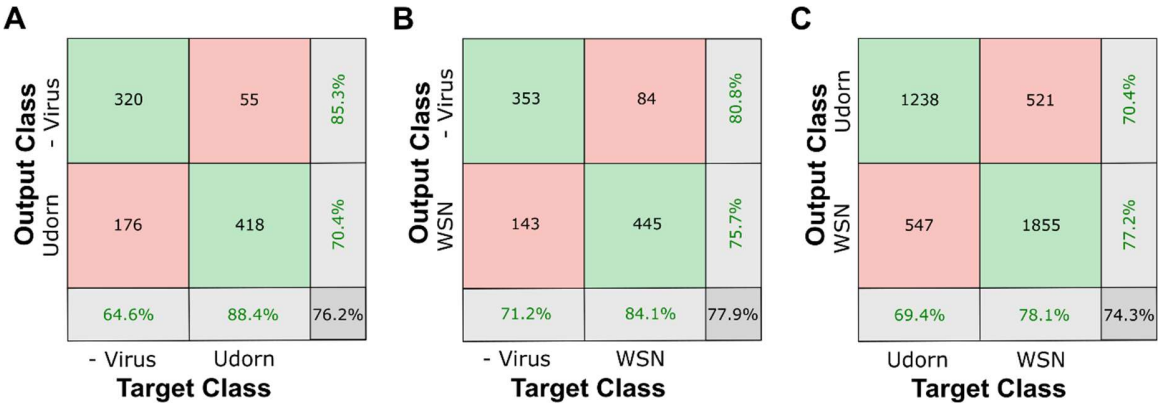

Sup. Fig. 6. Data taken on a Zeiss Elyra 7 shows similar results. A) Confusion matrix showing that a trained network could differentiate between Udorn and negative control. B) Confusion matrix showing that a trained network could differentiate between WSN and negative control. C) Confusion matrix showing that a trained network could differentiate between two strains of influenza (WSN and Udorn).

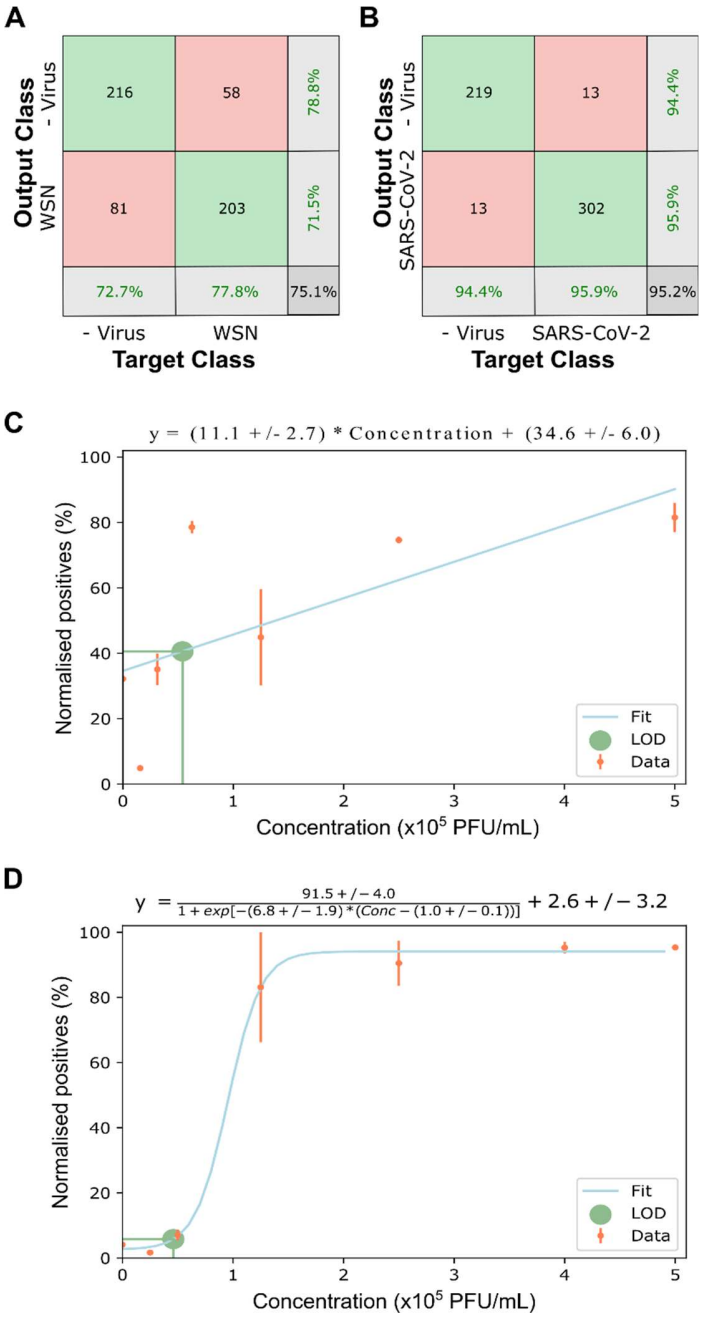

Sup. Fig. 7. Defining the limit of detection for influenza and SARS-CoV-2. A) Confusion matrix for a trained model distinguishing influenza strain A/WSN/33 vs. a minus virus control. B) Confusion matrix for SARS-CoV-2 vs. a minus virus control. C) Increasing concentrations of WSN were labelled and imaged, the resulting images were fed into the trained network. The number of normalised positive particles (positive particles/all particles) increased with increasing virus concentration. Error bars represent standard deviation. The limit of detection (LOD) was defined as 5.4×10^4 PFU/mL. D) As C), for SARS-CoV-2. The limit of detection (LOD) was defined as 4.6×10^4 PFU/mL.

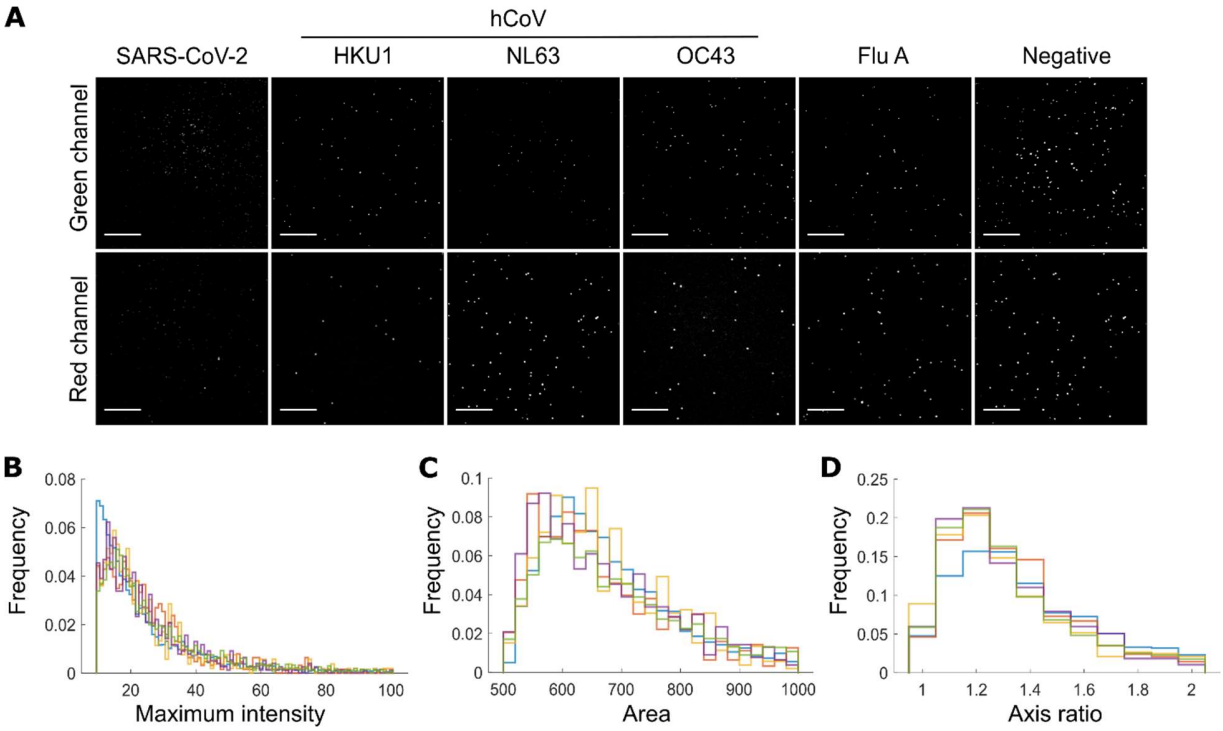

Sup. Fig. 8. Imaging comparison of clinical samples. A) Representative FOVs of fluorescently labelled SARS-CoV-2, three seasonal human coronaviruses hCoV, influenza A (Flu A) and a virus-negative control. The samples were immobilized and labelled with 0.23 M $CaCl_2$, 1 nM Cy3 (green) DNA and 1 nM Atto647N (red) DNA before being imaged. Scale bar 10µm. B-D) Normalised frequency plots of the maximum pixel intensity, area and semi-major-to-semi-minor-axis-ratio within the BBXs of five randomly selected SARS-CoV-2 clinical samples to show robustness and reproducibility of labelling. Values taken from 81 FOVs from a single slide for each virus, each sample depicted in a different colour.

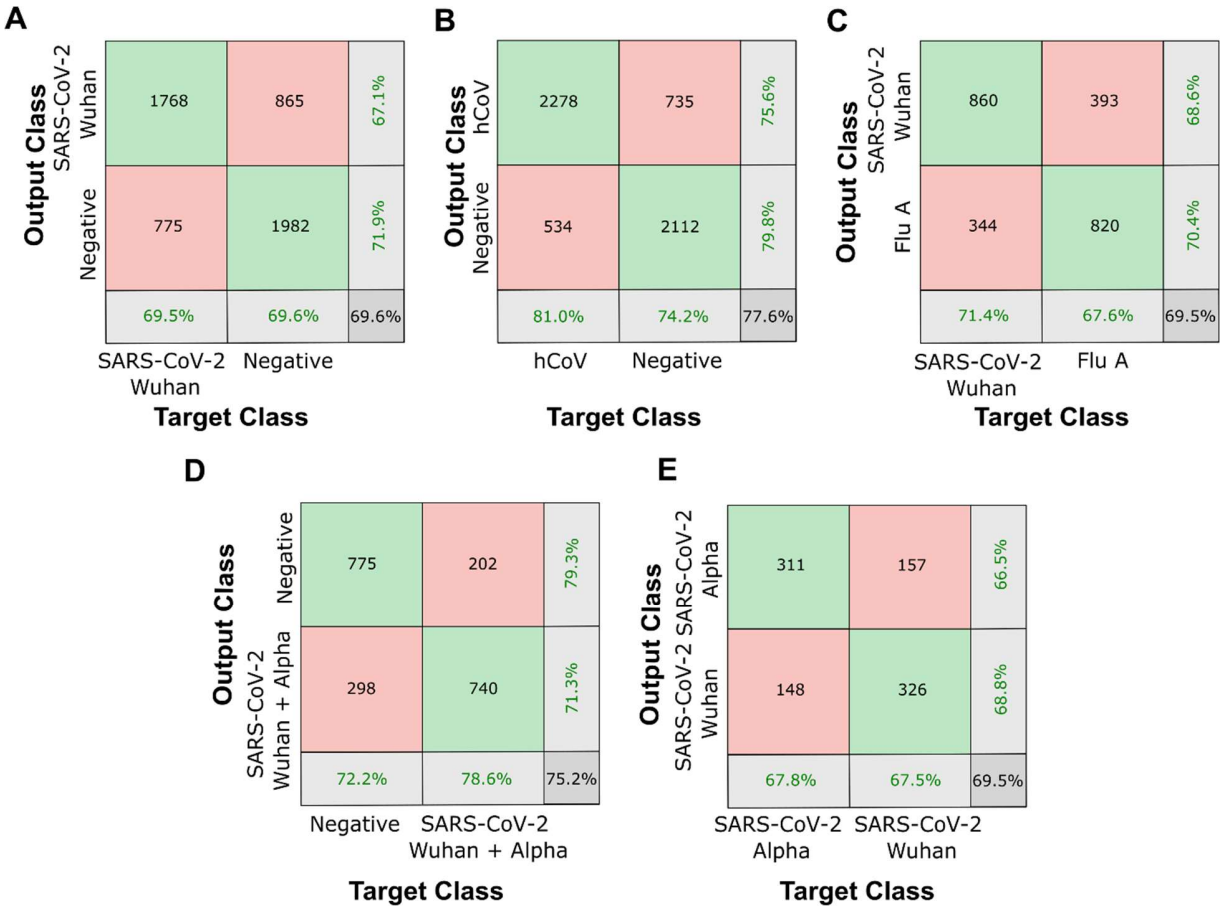

Sup. Fig. 9. Network validation results for clinical samples. A) Confusion matrix showing that a trained network could differentiate between SARS-CoV-2 Wuhan strain and negative samples. B) Confusion matrix showing that a trained network could differentiate between seasonal human coronaviruses hCoV and negative samples. C) Confusion matrix showing that a trained network could differentiate between clinical influenza A samples (Flu A) and SARS-CoV-2 Wuhan strain samples. D) Confusion matrix showing that a trained network could differentiate between two strains of SARS-CoV-2 (the original Wuhan strain and the Alpha variant) and negative samples. E) Confusion matrix showing that a trained network could differentiate between clinical samples of two variants of SARS-CoV-2, the original Wuhan strain (SARS-CoV-2 Wuhan) and the Alpha variant.

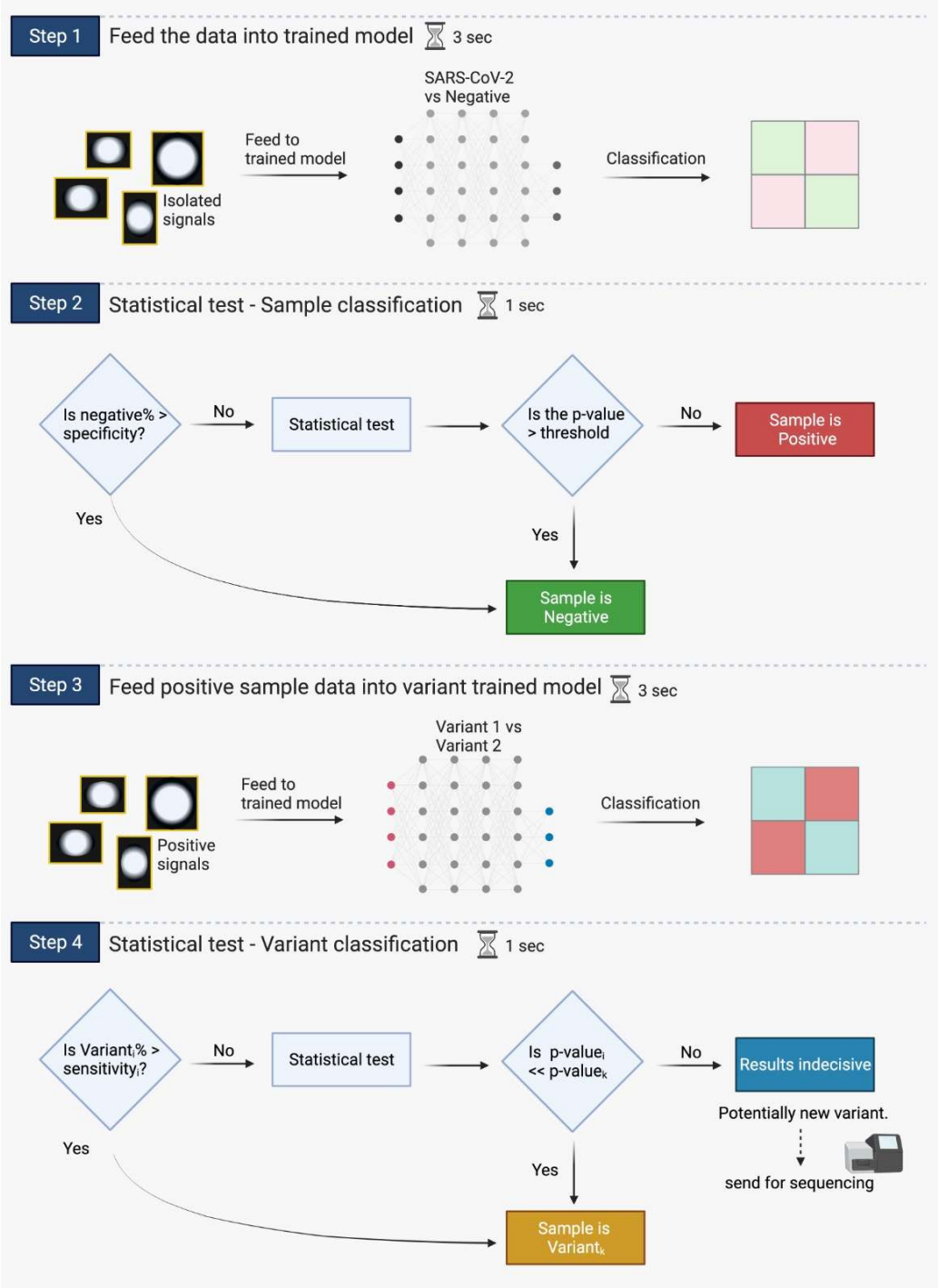

Sup. Fig. 10. Workflow for sample classification.
Step 1: Previously unseen samples are imaged, the images are processed into BBXs which are fed through a trained network (in this example, a network that has been trained to distinguish between SARS-CoV-2 and negative samples).
Step 2: Each sample is then classified:

- For each sample, if the percentage of BBXs classified as negative by the trained network (i.e. # negatives/total # of BBXs) is greater than the specificity of the trained model (given in step 3 of the first workflow above), then the sample is automatically classified as a negative.
- If not, then a chi-squared statistical test is performed, where we test the null hypothesis that the sample is negative. For the sample to be classified as positive we need a p-value smaller than our pre-set confidence threshold, in which case we can reject the null hypothesis and classify the sample as positive. If the p-value is greater than our threshold we cannot reject the null hypothesis and therefore the sample is classified as negative.

Step 3: If the sample is classified as SARS-CoV-2, the BBXs identified as positive from that sample can then be passed through a second trained network, in this case to test whether it is Covid-19 variant 1 or Covid-19 variant 2.

Step 4: Variant classification:

- For each sample, if the percentage of BBXs classified as positive by the trained network (i.e. # positives/total # of BBXs) for either variant is greater than the sensitivity for said variant, then the sample is classified as said variant.
- If not, then two chi squared tests are performed, each assuming as their null hypothesis that the sample is one of the two variants. The p-values are then calculated and compared. For a final variant classification, one of the p-values has to be at least 3 orders of magnitude smaller than the other, in which case the sample contains the variant with the bigger p-value. If the two p-values are closer than 3 orders of magnitude, the result is inconclusive, and the sample should be sent for sequencing.

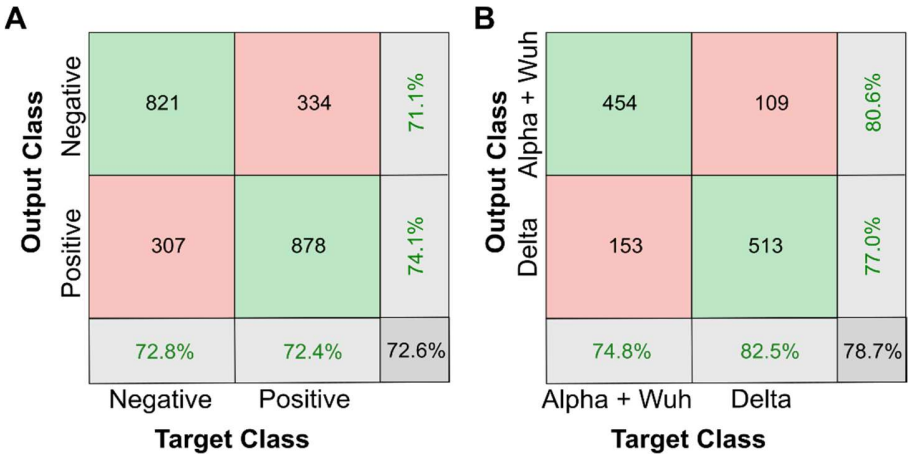

Sup. Fig. 11. Network validation results for clinical samples. A) Confusion matrix showing that a trained network could differentiate between SARS-CoV-2 positive and negative samples. B) Confusion matrix showing that a trained network could differentiate between the Delta SARS-CoV-2 variant and a combination of the Wuhan and Alpha variant strains of SARS-CoV-2.

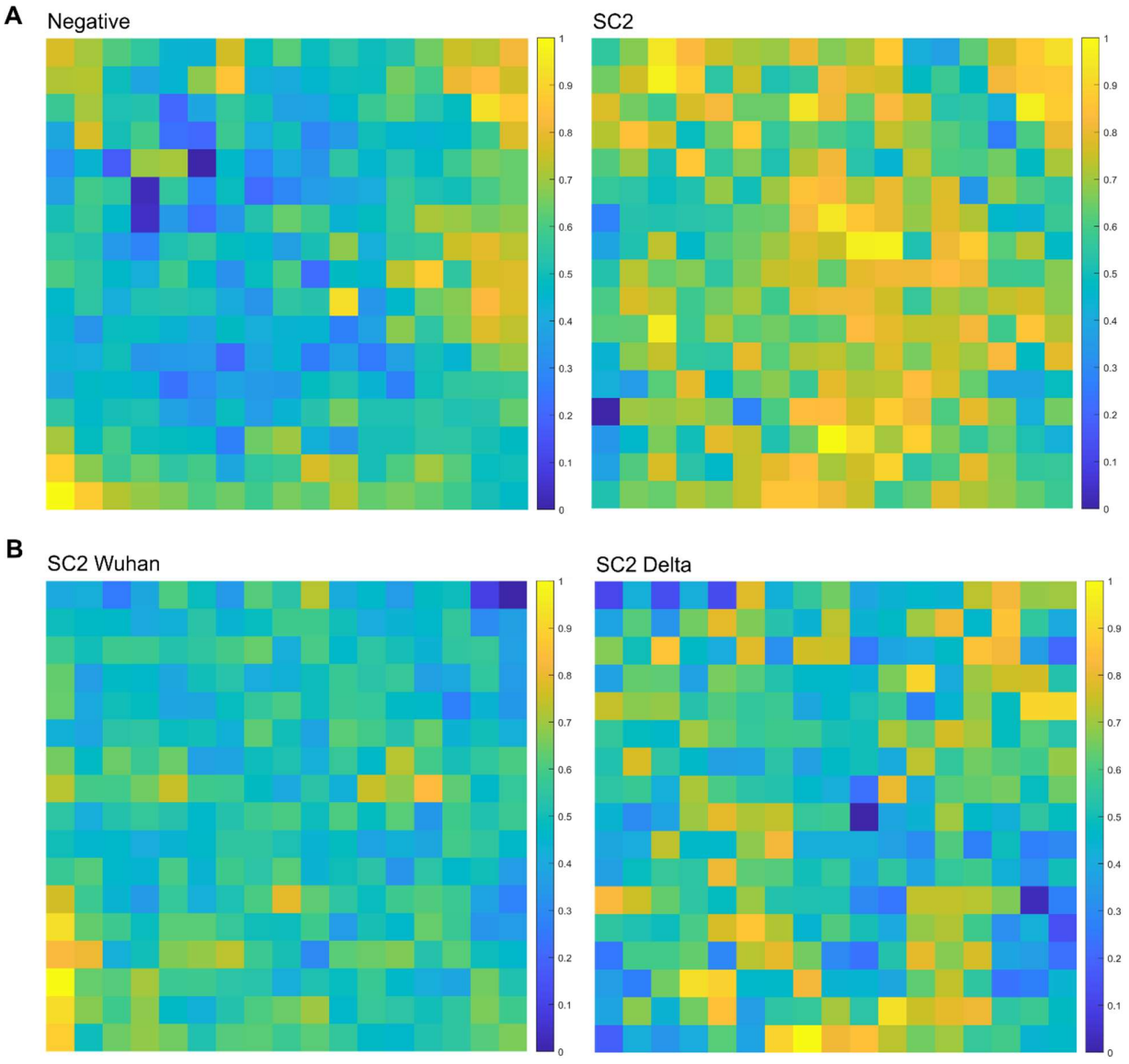

Sup. Fig. 12. Learned pattern visualisation by the convolutional neural network using the Matlab DeepDreamImage function. A) Patterns 'seen' by a network trained to differentiate between negative (left panel) and SARS-CoV-2 positive (SC2; right panel) samples. An image was forwarded through the network, and the gradient of the image with respect to the activations of a particular layer was calculated (in this case the fully connected layer). The image was modified to maximise these activations, enhancing the patterns 'seen' by the network. B) Patterns 'seen' by a network trained to differentiate between the original Wuhan variant strain of SARS-CoV-2 (SC2 Wuhan; left panel) and the Delta SARS-CoV-2 variant (SC2 Delta; right panel).

Table 1. Data on clinical samples used for training and validating the network. Multiple samples were imaged over three different days (described as -1, -2, -3 etc.). 70% of the BBXs generated over the three days were randomly selected for network training, while 30% were reserved for network validation (results depicted in the confusion matrices). Abbreviations used: hCoV – seasonal human coronaviruses (including the NL63, OC43 and HKU1 types), Neg – negative, SC2 – SARS-CoV-2 (original Wuhan variant), Flu A – Influenza A. 'Microscope 1' was a Nanoimager equipped with a Hamamatsu Flash 4 LT.1 sCMOS camera and 'Microscopes 2 and 3' were Nanoimagers equipped with a Hamamatsu Flash4 V3 sCMOS camera; in all other respects, the systems were identical.

Network	**hCoV vs Negative** (Microscope 1)					
	Identifier	**RT-PCR**	**Total # of BBXs**	**Identifier**	**RT-PCR**	**Total # of BBXs**
	T-Neg-1	Neg	1507	T-hCov-3-3	HKU1	148
	T-Neg-2	Neg	562	T-hCov-4	NL63	377
	T-Neg-3	Neg	451	T-hCov-4-1	NL63	80
	T-Neg-4	Neg	378	T-hCov-4-2	NL63	279
	T-Neg-1-1	Neg	5173	T-hCov-5	NL63	500
	T-Neg-2-1	Neg	122	T-hCov-5-1	NL63	513
	T-Neg-3-1	Neg	568	T-hCov-5-2	NL63	823
	T-Neg-4-1	Neg	158	T-hCov-6	NL63	453
	T-Neg-4-2	Neg	571	T-hCov-6-1	NL63	207
	T-hCov-1	HKU1	229	T-hCov-6-2	NL63	292
	T-hCov-1-1	HKU1	290	T-hCov-7	OC43	268
	T-hCov-1-2	HKU1	104	T-hCov-7-1	OC43	131
	T-hCov-1-3	HKU1	203	T-hCov-7-2	OC43	254
	T-hCov-2	HKU1	169	T-hCov-8	OC43	897
	T-hCov-2-1	HKU1	92	T-hCov-8-1	OC43	569
	T-hCov-2-2	HKU1	136	T-hCov-8-2	OC43	342
	T-hCov-3	HKU1	330	T-hCov-9	OC43	500
	T-hCov-3-1	HKU1	918	T-hCov-9-1	OC43	145
	T-hCov-3-2	HKU1	129			
					Total # of BBXs in dataset	18863
	SARS-CoV-2 Wuhan vs hCoV (Microscope 1)					
	Identifier	**RT-PCR**	**Total # of BBXs**	**Identifier**	**RT-PCR**	**Total # of BBXs**
	T-SC2-1	SC2	696	T-hCov-3-2	HKU1	129
	T-SC2-1-1	SC2	3320	T-hCov-3-3	HKU1	148
	T-SC-2	SC2	370	T-hCov-4	NL63	377
	T-SC-2-1	SC2	223	T-hCov-4-1	NL63	80
	T-SC-2-2	SC2	131	T-hCov-4-2	NL63	279
	T-SC-3	SC2	662	T-hCov-5	NL63	500
	T-SC-3-1	SC2	214	T-hCov-5-1	NL63	513
	T-SC-4	SC2	861	T-hCov-5-2	NL63	823
	T-SC-4-1	SC2	218	T-hCov-6	NL63	453
	T-SC-4-2	SC2	1783	T-hCov-6-1	NL63	207
	T-hCov-1	HKU1	229	T-hCov-6-2	NL63	292
	T-hCov-1-1	HKU1	290	T-hCov-7	OC43	268
	T-hCov-1-2	HKU1	104	T-hCov-7-1	OC43	131
	T-hCov-1-3	HKU1	203	T-hCov-7-2	OC43	254
	T-hCov-2	HKU1	169	T-hCov-8	OC43	897
	T-hCov-2-1	HKU1	92	T-hCov-8-1	OC43	569
	T-hCov-2-2	HKU1	136	T-hCov-8-2	OC43	342
	T-hCov-3	HKU1	330	T-hCov-9	OC43	500
	T-hCov-3-1	HKU1	918	T-hCov-9-1	OC43	145
					Total # of BBXs in dataset	17851
	SARS-CoV-2 Wuhan vs Negative (Microscope 1)					
	Identifier	**RT-PCR**	**Total # of BBXs**	**Identifier**	**RT-PCR**	**Total # of BBXs**
	T-SC2-1	SC2	696	T-SC-4-2	SC2	1783
	T-SC2-1-1	SC2	3320	T-Neg-1	Neg	1507
	T-SC-2	SC2	370	T-Neg-2	Neg	562
	T-SC-2-1	SC2	223	T-Neg-3	Neg	451

	T-SC-2-2	SC2	131	T-Neg-4	Neg	378
	T-SC-3	SC2	662	T-Neg-1-1	Neg	5173
	T-SC-3-1	SC2	214	T-Neg-2-1	Neg	122
	T-SC-4	SC2	861	T-Neg-3-1	Neg	568
	T-SC-4-1	SC2	218	T-Neg-4-1	Neg	729
					Total # of BBXs in dataset	17968
	Flu A vs Negative (Microscope 1)					
	Identifier	**RT-PCR**	**Total # of BBXs**	**Identifier**	**RT-PCR**	**Total # of BBXs**
	T-Neg-5	Neg	514	T-Neg-4	Neg	378
	T-Neg-5-1	Neg	337	T-Neg-4-1	Neg	158
	T-Neg-5-2	Neg	471	T-Neg-4-2	Neg	571
	T-Neg-2	Neg	652	T-Neg-4-3	Neg	154
	T-Neg-2-1	Neg	77	T-Neg-4-4	Neg	233
	T-Neg-2-2	Neg	45	T-FluA-1	Flu A	1782
	T-Neg-2-3	Neg	242	T-FluA-1-1	Flu A	289
	T-Neg-3	Neg	451	T-FluA-1-2	Flu A	246
	T-Neg-3-1	Neg	568	T-FluA-2	Flu A	61
	T-Neg-3-2	Neg	398	T-FluA-2-1	Flu A	658
	T-Neg-3-3	Neg	150	T-FluA-3	Flu A	1177
	T-Neg-3-4	Neg	374			
					Total # of BBXs in dataset	10461
	SARS-COV-2 Wuhan vs Flu A (Microscope 1)					
	Identifier	**RT-PCR**	**Total # of BBXs**	**Identifier**	**RT-PCR**	**Total # of BBXs**
	T-FluA-5	Flu A	289	T-SC-2-1	SC2	**223**
	T-FluA-5-1	Flu A	246	T-SC-2-3	SC2	318
	T-FluA-5-2	Flu A	2416	T-SC-4-3	SC2	122
	T-FluA-6	Flu A	188	T-SC-4-4	SC2	200
	T-FluA-6-1	Flu A	748	T-SC-4-5	SC2	546
	T-FluA-6-2	Flu A	158	T-SC-5	SC2	170
	T-SC2-1-2	SC2	248	T-SC-5-1	SC2	260
	T-SC2-1-3	SC2	209	T-SC-5-2	SC2	630
	T-SC2-1-4	SC2	236	T-SC-5-3	SC2	823
					Total # of BBXs in dataset	8060
	SARS-CoV-2 Alpha vs SARS-CoV-2 Wuhan (Microscope 2)					
	Identifier	**RT-PCR**	**Total # of BBXs**	**Identifier**	**RT-PCR**	**Total # of BBXs**
	T-SC2-6	B.1.1.7	631	T-SC2-9	SC2	483
	T-SC2-7	B.1.1.7	663	T-SC2-10	SC2	511
	T-SC2-8	B.1.1.7	235	T-SC2-11	SC2	616
					Total # of BBXs in dataset	3139
	SARS-CoV-2 (Wuhan and Alpha) vs Negative (Microscope 2)					
	Identifier	**RT-PCR**	**Total # of BBXs**	**Identifier**	**RT-PCR**	**Total # of BBXs**
	T-SC2-6	B.1.17	631	T-SC2-11	SC2	616
	T-SC2-12	B.1.1.7	127	T-Neg-5	Neg	655
	T-SC2-13	B.1.1.7	771	T-Neg-6	Neg	1318
	T-SC2-9	SC2	483	T-Neg-7	Neg	595
	T-SC2-10	SC2	511	T-Neg-8	Neg	1008
					Total # of BBXs in dataset	6715
	SARS-CoV-2 Alpha vs Negative (Microscope 2)					
	Identifier	**RT-PCR**	**Total # of BBXs**	**Identifier**	**RT-PCR**	**Total # of BBXs**
	T-SC-2-6	B.1.1.7	631	T-Neg-5	Neg	655
	T-SC-2-7	B.1.1.7	663	T-Neg-7	Neg	469
	T-SC-2-8	B.1.1.7	235	T-Neg-9	Neg	595
					Total # of BBXs in dataset	3248
	SARS-CoV-2 vs Negative (Microscope 3)					
	Identifier	**RT-PCR**	**Total # of BBXs**	**Identifier**	**RT-PCR**	**Total # of BBXs**
	NEG-J-2	Negative	792	NEG-J-30	Negative	310
	NEG-J-3	Negative	135	SC2-WT-02	SARS-CoV-2	483
	NEG-J-4	Negative	182	SC2-WT-07	SARS-CoV-2	511
	NEG-J-5	Negative	451	SC2-WT-13	SARS-CoV-2	616
	NEG-J-6	Negative	672	SC2-D-2	SARS-CoV-2	500
	NEG-J-12	Negative	1218	SC2 lab grown	N/A	582
					Total # of BBXs in dataset	6452
	Wuhan + Alpha vs Delta variant (Microscope 3)					

	Identifier	RT-PCR	Total # of BBXs	Identifier	RT-PCR	Total # of BBXs
	SC2-A-01	SARS-CoV-2	360	SC2-D-3	SARS-CoV-2	31
	SC2-A-03	SARS-CoV-2	188	SC2-D-4	SARS-CoV-2	9
	SC2-A-09	SARS-CoV-2	1022	SC2-D-9	SARS-CoV-2	266
	SC2-WT-04	SARS-CoV-2	491	SC2-D-10	SARS-CoV-2	81
	SC2-WT-05	SARS-CoV-2	572	SC2-D-12	SARS-CoV-2	455
	SC2-WT-11	SARS-CoV-2	460	SC2-D-13	SARS-CoV-2	236
	SC2-D-1	SARS-CoV-2	1680	SC2-D-29	SARS-CoV-2	536
					Total # of BBXs in dataset	6387

Table 2. Results of independent testing of the network on samples not seen before (51 samples). Abbreviations used: hCoV – seasonal human coronaviruses (including the NL63, OC43 and HKU1 types), Neg – negative, na – statistical test not needed as the percentage of BBXs classified as negative by the trained network (i.e. # negatives/total # of BBXs) is greater than the specificity of the trained model, SC2 – SARS-CoV-2, Flu A – Influenza A, SC2-S0 – SARS-CoV-2 spike gene target failure in RT-PCR indicative of the Alpha variant. Incorrectly classified sample highlighted in turquoise.

Network	Identifier	RT-PCR		Total # of BBXs		P-value	Result
'Microscope 1'				hCov	Negative	Threshold: 0.01	
hCoV vs Negative	hCoV-1	NL63	6467	4271	2196	5.18E-10	hCoV
	hCoV-2	NL63	2672	1307	1365	5.184-21	hCoV
	hCoV-3	NL63	227	111	116	0.006	hCoV
	hCoV-4	OC43	2239	1706	533	9.25E-268	hCoV
	hCoV-5	OC43	653	442	211	2.80E-47	hCoV
	hCoV-6	OC43	840	555	285	1.13E-53	hCoV
	hCoV-7	HKU1	1342	1087	255	2.09E-206	hCoV
	hCoV-8	HKU1	1898	1069	829	9.69E-48	hCoV
	hCoV-9	HKU1	6745	3797	2948	2.82E-164	hCoV
	NEG-1	Neg	514	198	316	0.49	Neg
	NEG-2	Neg	398	141	257	na	Neg
	NEG-3	Neg	154	29	125	na	Neg
'Microscope 1'				SC2	hCov	Threshold: 0.01	
SARS-CoV-2 Wuhan vs hCoV	SC2-1	SARS-CoV-2	5589	3653	1936	5.18E-10	SC2
	SC2-2	SARS-CoV-2	1762	1312	450	5.14E-21	SC2
	SC2-3	SARS-CoV-2	284	86	198	0.917	hCoV
	hCoV-7	HKU1	1342	159	1183	na	hCoV
	hCoV-8	HKU1	1898	593	1305	0.237	hCoV
	hCoV-10	HKU1	3182	654	2528	na	hCoV
	hCoV-11	OC43	264	8	256	na	hCoV
	hCoV-12	OC43	479	21	458	na	hCoV
	hCoV-13	OC43	7966	2245	5721	na	hCoV
	hCoV-14	NL63	305	12	293	na	hCoV
	hCoV-15	NL63	968	89	879	na	hCoV
	hCoV-16	NL63	2269	349	1920	na	hCoV
'Microscope 1'				SC2	Neg	Threshold: 0.01	
SARS-CoV-2 Wuhan vs Negative	SC2-4	SARS-CoV-2	200	150	50	7.93E-21	SC2
	SC2-5	SARS-CoV-2	560	503	57	1.07E-114	SC2
	SC2-6	SARS-CoV-2	529	496	33	7.58E-127	SC2
	SC2-7	SARS-CoV-2	173	148	25	1.11E-30	SC2
	SC2-8	SARS-CoV-2	150	135	15	2.89E-32	SC2
	SC2-9	SARS-CoV-2	8095	3575	4520	6.91E-4	SC2
	Neg-4	Neg	158	28	130	na	Neg
	Neg-5	Neg	568	240	328	0.982	Neg
	Neg-6	Neg	77	16	61	na	Neg
	Neg-7	Neg	337	132	215	na	Neg
'Microscope 1'				Flu A	Neg	Threshold: 0.01	
Flu A vs Negative	Flu A -1	Flu A	311	263	48	2.08E-08	Flu A
	Flu A -2	Flu A	195	163	32	3.46E-05	Flu A
	Flu A -3	Flu A	24383	24231	152	0.00	Flu A
	Flu A -4	Flu A	212	185	27	4.13E-08	Flu A
	Neg-8	Neg	1507	41	1466	na	Neg
	Neg-9	Neg	374	259	115	0.22	Neg
	Neg-10	Neg	354	235	119	0.14	Neg
'Microscope 1'				SC2	Flu A	Threshold: 0.01	
SARS-CoV-2 Wuhan vs Flu A	SC2-10	SARS-CoV-2	1783	1551	232	0.00	SC2
	SC2-11	SARS-CoV-2	1340	818	522	2.54E-81	SC2
	SC2-12	SARS-CoV-2	13915	5413	8502	3.40E-21	SC2
	Flu A -1	Flu A	311	106	205	na	Flu A

	Flu A -2	Flu A	195	53	142	0.270		Flu A
	Flu A -3	Flu A	24383	2871	21512	na		Flu A
	Flu A -4	Flu A	212	51	161	na		Flu A
'Microscope 2'				B.1.1.7	Negative	Threshold: 0.01		
SARS-CoV-2 Alpha vs Negative	SC2-13	SC2-S0	4979	2538	2441	0.00		B.1.1.7
	SC2-14	SC2-S0	631	602	29	0.00		B.1.1.7
	SC2-15	SC2-S0	127	117	10	2.18E-61		B.1.1.7
	SC2-16	SC2-S0	771	738	33	0.00		B.1.1.7
	Neg-8	Neg	4166	22	4144	na		Neg
	Neg-9	Neg	2888	130	2758	na		Neg
	Neg-10	Neg	3369	947	2422	0.147		Neg
'Microscope 2'				SC2	Negative	Threshold: 0.01		
SARS-CoV-2 (Wuhan + Alpha) vs Negative	SC2-17	SC2-S0	5024	2309	2715	0.000		SC2
	SC2-14	SC2-S0	631	563	68	0.000		SC2
	SC2-15	SC2-S0	127	97	30	0.000		SC2
	SC2-16	SC2-S0	771	709	62	0.000		SC2
	SC2-18	SC2-S0	2492	2254	238	0.000		SC2
	SC2-19	SC2	4058	1302	2756	0.004		SC2
	SC2-20	SC2	1609	1410	199	0.000		SC2
	Neg-8	Neg	4166	33	4133	na		Neg
	Neg-9	Neg	2888	164	2724	na		Neg
	Neg-10	Neg	2422	32	2390	na		Neg
	Neg-11	Neg	2435	741	1694	0.64		Neg
'Microscope 2'				SC2	B.1.1.7	p-SC2	p-B.1.1.7	
SARS-CoV-2 Alpha vs SARS-CoV-2 Wuhan	SC2-17	SC2-S0	2309	981	1328	1.683E-138	3.20E-22	B.1.1.7
	SC2-14	SC2-S0	563	116	447	3.21E-121	4.06E-13	B.1.1.7
	SC2-15	SC2-S0	97	33	64	4.92E-12	0.831	B.1.1.7
	SC2-16	SC2-S0	709	155	554	4.17E-144	2.84E-10	B.1.1.7
	SC2-18	SC2-S0	2254	1051	1203	5.21E-94	4.43E-43	B.1.1.7
	SC2-19	SC2	1302	725	577	3.82E-18	7.31E-68	SC2
	SC2-20	SC2	1410	776	634	1.24E-21	2.60E-69	SC2

Table 3. Results of independent testing of the network on samples not seen before (104 samples). Abbreviations used: Neg – negative, NA – statistical test not needed as the percentage of BBXs classified as negative by the trained network (i.e. # negatives/total # of BBXs) is greater than the specificity of the trained model, SC2 – SARS-CoV-2. Samples with less than the 5 BBXs needed for the chi-squared test are highlighted in yellow and incorrectly classified samples are highlighted in turquoise.

Network	Identifier	RT-PCR	# of BBXs			P-value	Result
'Microscope 3'			Total	SC2	Negative	Threshold: 0.012	
SARS-CoV-2 vs Negative	**Neg-2-01**	**Negative**	**41**	**1**	**40**	**NA**	**NEGATIVE**
	Neg-2-02	Negative	434	71	363	NA	NEGATIVE
	Neg-2-03	Negative	820	154	666	NA	NEGATIVE
	Neg-2-04	Negative	1126	228	898	NA	NEGATIVE
	Neg-2-05	Negative	716	135	581	NA	NEGATIVE
	Neg-2-06	Negative	1390	363	1027	NA	NEGATIVE
	Neg-2-07	Negative	891	250	641	NA	NEGATIVE
	Neg-2-08	Negative	1763	491	1272	NA	NEGATIVE
	Neg-2-09	Negative	235	33	202	NA	NEGATIVE
	Neg-J-02	Negative	922	145	777	NA	NEGATIVE
	Neg-J-03	Negative	274	42	232	NA	NEGATIVE
	Neg-J-04	Negative	182	31	151	NA	NEGATIVE
	Neg-J-05	Negative	1078	139	939	NA	NEGATIVE
	Neg-J-06	Negative	932	124	808	NA	NEGATIVE
	Neg-J-07	Negative	1383	181	1202	NA	NEGATIVE
	Neg-J-08	Negative	571	117	454	NA	NEGATIVE
	Neg-J-09	Negative	768	116	652	NA	NEGATIVE
	Neg-J-10	Negative	759	97	662	NA	NEGATIVE
	Neg-J-11	Negative	154	29	125	NA	NEGATIVE
	NEG-J-12	Negative	1341	428	913	0.468048338	NEGATIVE
	Neg-J-13	Negative	988	294	694	NA	NEGATIVE
	Neg-J-14	Negative	4	3	1	INCONCLUSIVE	INCONCLUSIVE
	Neg-J-15	Negative	897	286	611	0.566986783	NEGATIVE
	Neg-J-16	Negative	248	48	200	NA	NEGATIVE
	Neg-J-17	Negative	65	14	51	NA	NEGATIVE
	Neg-J-18	Negative	156	14	142	NA	NEGATIVE
	Neg-J-19	Negative	216	31	185	NA	NEGATIVE
	Neg-J-20	Negative	1163	392	771	0.04601353	NEGATIVE
	Neg-J-21	Negative	634	144	490	NA	NEGATIVE
	Neg-J-22	Negative	53	13	40	NA	NEGATIVE
	Neg-J-23	Negative	218	33	185	NA	NEGATIVE
	Neg-J-24	Negative	580	155	425	NA	NEGATIVE
	Neg-J-25	Negative	456	121	335	NA	NEGATIVE
	Neg-J-26	Negative	567	135	432	NA	NEGATIVE
	Neg-J-27	Negative	377	72	305	NA	NEGATIVE
	Neg-J-28	Negative	243	57	186	NA	NEGATIVE
	Neg-J-29	Negative	1257	508	749	5.34E-13	POSITIVE
	Neg-J-30	Negative	310	44	266	NA	NEGATIVE
	Neg-J-31	Negative	46	7	39	NA	NEGATIVE
	Neg-J-32	Negative	119	14	105	NA	NEGATIVE
	Neg-J-33	Negative	316	75	241	NA	NEGATIVE
	Neg-J-34	Negative	1593	445	1148	NA	NEGATIVE
	Neg-J-36	Negative	973	185	788	NA	NEGATIVE
	Neg-J-37	Negative	46	6	40	NA	NEGATIVE
	Neg-J-38	Negative	521	71	450	NA	NEGATIVE
	Neg-J-39	Negative	1495	357	1138	NA	NEGATIVE
	Neg-J-40	Negative	1026	249	777	NA	NEGATIVE
	Neg-J-41	Negative	73	11	62	NA	NEGATIVE
	Neg-J-42	Negative	985	304	681	NA	NEGATIVE
	NEG-J-43	Negative	1	0	1	INCONCLUSIVE	INCONCLUSIVE
	NEG-J-44	Negative	14	2	12	NA	NEGATIVE

	NEG-J-45	Negative	7	0	7	NA	NEGATIVE
	NEG-J-46	Negative	30	1	29	NA	NEGATIVE
	NEG-J-47	Negative	33	3	30	NA	NEGATIVE
	NEG-J-48	Negative	12	0	12	NA	NEGATIVE
	NEG-J-49	Negative	24	1	23	NA	NEGATIVE
	NEG-J-50	Negative	14	0	14	NA	NEGATIVE
	NEG-J-51	Negative	22	0	22	NA	NEGATIVE
	NEG-J-52	Negative	8	0	8	NA	NEGATIVE
	NEG-J-53	Negative	39	1	38	NA	NEGATIVE
	NEG-J-55	Negative	26	0	26	NA	NEGATIVE
	NEG-J-56	Negative	16	1	15	NA	NEGATIVE
	NEG-J-57	Negative	18	2	16	NA	NEGATIVE
	NEG-J-58	Negative	29	4	25	NA	NEGATIVE
	NEG-J-59	Negative	1068	298	770	NA	NEGATIVE
	Neg-J-60	Negative	267	54	213	NA	NEGATIVE
	NEG-J-61	Negative	1307	377	930	NA	NEGATIVE
	Neg-J-62	Negative	1419	384	1035	NA	NEGATIVE
	SC2-A-01	SARS-CoV-2	2492	1654	838	0	POSITIVE
	SC2-A-02	SARS-CoV-2	5024	4663	361	0	POSITIVE
	SC2-A-03	SARS-CoV-2	2214	806	1408	3.83E-08	POSITIVE
	SC2-A-04	SARS-CoV-2	490	172	318	0.049608197	NEGATIVE
	SC2-A-05	SARS-CoV-2	931	826	105	0	POSITIVE
	SC2-A-06	SARS-CoV-2	4118	4045	73	0	POSITIVE
	SC2-A-07	SARS-CoV-2	127	99	28	2.61E-30	POSITIVE
	SC2-A-08	SARS-CoV-2	771	559	212	4.81E-137	POSITIVE
	SC2-A-09	SARS-CoV-2	3265	3252	13	0	POSITIVE
	SC2-A-10	SARS-CoV-2	313	144	169	9.44E-09	POSITIVE
	SC2-A-11	SARS-CoV-2	1367	494	873	4.01E-05	POSITIVE
	SC2-A-12	SARS-CoV-2	68	38	30	9.14E-06	POSITIVE
	SC2-D-01	SARS-CoV-2	8351	8342	9	0	POSITIVE
	SC2-D-03	SARS-CoV-2	1191	945	246	5.65E-285	POSITIVE
	SC2-D-04	SARS-CoV-2	2315	2159	156	0	POSITIVE
	SC2-D-09	SARS-CoV-2	348	266	82	5.04E-75	POSITIVE
	SC2-D-10	SARS-CoV-2	324	81	243	NA	NEGATIVE
	SC2-D-12	SARS-CoV-2	1163	455	708	2.10E-09	POSITIVE
	SC2-D-13	SARS-CoV-2	660	236	424	0.008224134	POSITIVE
	SC2-D-25	SARS-CoV-2	337	126	211	0.011217453	POSITIVE
	SC2-D-28	SARS-CoV-2	1510	771	739	9.79E-64	POSITIVE
	SC2-D-29	SARS-CoV-2	1347	1052	295	9.54E-306	POSITIVE
	SC2-WT-01	SARS-CoV-2	4058	3895	163	0	POSITIVE
	SC2-WT-02	SARS-CoV-2	1609	1149	460	4.10E-269	POSITIVE
	SC2-WT-03	SARS-CoV-2	1281	1123	158	0	POSITIVE
	SC2-WT-04	SARS-CoV-2	1206	830	376	2.02E-177	POSITIVE
	SC2-WT-05	SARS-CoV-2	2043	1740	303	0	POSITIVE
	SC2-WT-06	SARS-CoV-2	1332	1264	68	0	POSITIVE
	SC2-WT-07	SARS-CoV-2	2777	2736	41	0	POSITIVE
	SC2-WT-08	SARS-CoV-2	860	437	423	3.35E-36	POSITIVE
	SC2-WT-09	SARS-CoV-2	2130	2126	4	0	POSITIVE
	SC2-WT-10	SARS-CoV-2	1600	1411	189	0	POSITIVE
	SC2-WT-11	SARS-CoV-2	1671	1311	360	0	POSITIVE
	SC2-WT-12	SARS-CoV-2	2301	1862	439	0	POSITIVE
	SC2-WT-13	SARS-CoV-2	2808	2252	556	0	POSITIVE
	SC2-WT-14	SARS-CoV-2	4295	4286	9	0	POSITIVE

Table 4. Results of variant classification (35 samples). Abbreviations used: Neg – negative, NA – statistical test not needed as the percentage of BBXs classified as positive by the trained network (i.e. # positives/total # of BBXs) for either variant is greater than the sensitivity for said variant, then the sample is classified as said variant, SC2 – SARS-CoV-2. Samples with p-values closer than 3 orders of magnitude (i.e. inconclusive) are highlighted in yellow and incorrectly classified samples are highlighted in turquoise.

Network	Identifier	RT-PCR	BBXs breakdown			P-value		Result
'Microscope 3'			Total # of BBXs	A+WT	D	P-A+WT Null hypothesis A+WT	P-D Null hypothesis D	
SARS-CoV-2 Alpha+Wuhan vs SARS-CoV-2 Delta	NEG-J-29	Negative	508	325	183	9.58385E-09	1.30046E-21	Delta
	SC2-D-01	Delta Variant	8342	409	7933	0	NA	Delta
	SC2-D-03	Delta Variant	31	30	1	NA	1.47E-09	Alpha-Wuhan
	SC2-D-04	Delta Variant	9	4	5	0.03426401	0.930251279	Inconclusive
	SC2-D-09	Delta Variant	266	133	133	4.67E-21	0.021108289	Delta
	SC2-D-12	Delta Variant	455	223	232	1.59E-37	0.009600884	Delta
	SC2-D-13	Delta Variant	236	128	108	1.76E-13	0.000488561	Delta
	SC2-D-25	Delta Variant	337	109	228	4.27E-73	NA	Delta
	SC2-D-28	Delta Variant	771	549	222	0.01498451	2.27E-56	Alpha-Wuhan
	SC2-D-29	Delta Variant	1052	184	868	0	NA	Delta
	SC2-S0-01	Wuhan/Alpha Variant	1654	1248	406	NA	1.38E-156	Alpha-Wuhan
	SC2-S0-02	Wuhan/Alpha Variant	4663	4513	150	NA	0	Alpha-Wuhan
	SC2-S0-03	Wuhan/Alpha Variant	806	672	134	NA	1.36E-118	Alpha-Wuhan
	SC2-S0-05	Wuhan/Alpha Variant	526	476	50	NA	2.75E-107	Alpha-Wuhan
	SC2-S0-06	Wuhan/Alpha Variant	4045	3530	515	NA	0	Alpha-Wuhan
	SC2-S0-07	Wuhan/Alpha Variant	99	89	10	NA	4.28E-21	Alpha-Wuhan
	SC2-S0-08	Wuhan/Alpha Variant	559	529	30	NA	2.99E-134	Alpha-Wuhan
	SC2-S0-09	Wuhan/Alpha Variant	3252	3051	201	NA	0	Alpha-Wuhan
	SC2-S0-10	Wuhan/Alpha Variant	144	72	72	4.26219E-12	0.089751493	Delta
	SC2-S0-11	Wuhan/Alpha Variant	494	147	347	2.68E-119	NA	Delta
	SC2-S0-12	Wuhan/Alpha Variant	38	22	16	0.01488672	0.063651707	Inconclusive
	SC2-WT-01	Wuhan/Alpha Variant	3895	3740	155	NA	0	Alpha-Wuhan
	SC2-WT-02	Wuhan/Alpha Variant	1149	868	281	NA	5.50E-110	Alpha-Wuhan
	SC2-WT-03	Wuhan/Alpha Variant	1123	1025	98	NA	3.45E-234	Alpha-Wuhan
	SC2-WT-04	Wuhan/Alpha Variant	830	770	60	NA	1.92E-184	Alpha-Wuhan
	SC2-WT-05	Wuhan/Alpha Variant	1740	1541	199	NA	0	Alpha-Wuhan
	SC2-WT-06	Wuhan/Alpha Variant	1264	1190	74	NA	2.51E-295	Alpha-Wuhan
	SC2-WT-07	Wuhan/Alpha Variant	2736	2516	220	NA	0	Alpha-Wuhan
	SC2-WT-08	Wuhan/Alpha Variant	860	501	359	8.32E-30	1.61E-19	Delta
	SC2-WT-09	Wuhan/Alpha Variant	2126	574	1552	0	NA	Delta

	SC2-WT-10	Wuhan/Alpha Variant	1411	1317	94	NA	0	Alpha-Wuhan
	SC2-WT-11	Wuhan/Alpha Variant	1311	1221	90	NA	2.49E-294	Alpha-Wuhan
	SC2-WT-12	Wuhan/Alpha Variant	1862	1590	272	NA	7.56E-299	Alpha-Wuhan
	SC2-WT-13	Wuhan/Alpha Variant	2252	1895	357	NA	0	Alpha-Wuhan
	SC2-WT-14	Wuhan/Alpha Variant	4286	3696	590	NA	0	Alpha-Wuhan